OPEN

Corneal Epithelial Thickness Mapping in the Diagnosis of Ocular Surface Disorders Involving the Corneal Epithelium: A Comparative Study

Arielle Levy, MD, Cristina Georgeon, Juliette Knoeri, MD, Moïse Tourabaly, MD, Loïc Leveziel, MD, Nacim Bouheraoua, MD, PhD, and Vincent M. Borderie, MD, PhD

Purpose: The purpose of this study was to analyze the role of corneal epithelial thickness (ET) mapping provided by spectral domain optical coherence tomography in the diagnosis of ocular surface disorders (OSDs) involving the corneal epithelium.

Design: This was a retrospective comparative study.

Methods: Institutional settings are as follows. Study population includes 303 eyes with an OSD and 55 normal eyes (controls). Observation procedures include spectral domain optical coherence tomography with epithelial mapping in the central 6 mm. Main outcome measures include ET map classification (normal, doughnut, spoke-wheel, localized/diffuse, and thinning/thickening patterns) and ET data and statistics (minimum, maximum, and SD). A quantitative threshold was determined with receiver operating curves to distinguish pathological from normal corneas. Sensitivity and specificity of classification and quantitative data were calculated using all eyes to assess the ability to distinguish corneas with a given corneal disorder from other conditions.

Results: Classification of full agreement between 3 readers was obtained in 75.4% to 99.4% of cases. Main OSD features were keratoconus (135 eyes), doughnut pattern (sensitivity/specificity = 56/94%), and max–min ET $\geq$ 13 μm (84/43%); limbal deficiency (56 eyes), spoke-wheel pattern (66/98%), and max–min ET $\geq$ 14 μm (91/59%); epithelial basement membrane dystrophy (55 eyes), inferior thickening pattern (55/92%), and central ET $>$ 56 μm (53/81%); dry eye (21 eyes), superior thinning pattern (67/88%), and minimal ET $\leq$ 44 μm (86/48%); pterygium (10 eyes), nasal thickening pattern (100/86%), and nasal ET $>$ 56 μm (80/71%); and in situ carcinoma (11 eyes), max ET $>$ 60 μm (91/60%), and ET SD $>$5 μm (100/58%).

Conclusions: The epithelial map pattern recognition combined with quantitative analysis of ET is relevant for the diagnosis of OSDs and for distinguishing various OSDs from each other. Deep learning analysis of big data could lead to the fully automated diagnosis of these disorders.

Key Words: dry eye, epithelial basement membrane dystrophy, in situ carcinoma, keratoconus, limbal deficiency, optical coherence tomography, pterygium

(*Cornea* 2022;41:1353–1361)

The corneal epithelium serves as a barrier to the outside environment and, in concert with the tear film, plays an essential role in the refractive power of the eye. It features 5 to 7 cell layers and an average central thickness ranging from 50 to 52 μm. Its thickness is not always homogeneous, and it tends to compensate for the irregular stromal surface.[1] Reinstein et al described how the epithelial thickness (ET) profile remodels in response to stromal irregularities.[2,3] This theory was first proposed by Vogt[4] in 1962 who mentioned that "corneal stromal defects are filled with surface epithelial cells."

Therefore, the analysis of corneal ET may play a key role in the early diagnosis and evaluation of different ocular surface disorders.[5] For instance, in keratoconus eyes, focal epithelial thinning may be an early disease indicator and the ET in the thinnest corneal zone is an indicator of forme fruste keratoconus.[6,7] Several studies have reported the features of corneal ET in individual diseases, such as epithelial basement membrane dystrophy (EBMD),[8] limbal stem cell deficiency (LSCD),[9,10] keratoconus, and dry eye.[11] However, to the best of our knowledge, no studies have referred the value of corneal ET as a test complementary to clinical evaluation in the diagnosis and differentiation of these diseases altogether, especially in difficult situations.

Epithelial and stromal thicknesses have been measured with several devices including high-frequency scanning ultrasound biomicroscopy, in vivo confocal microscopy (IVCM), and spectral domain optical coherence tomography (SD-OCT). IVCM[11,12] and high-frequency scanning ultrasound biomicroscopy[13,14] are invasive contact techniques. SD-OCT is a noncontact technique based on the principles of

Received for publication June 20, 2021; revision received October 25, 2021; accepted December 5, 2021. Published online ahead of print March 30, 2022.

From the GRC 32, Transplantation et Thérapies Innovantes de la Cornée, Sorbonne Université, Centre Hospitalier National d'Ophtalmologie des Quinze-Vingts, Paris, France.

The authors have no funding or conflicts of interest to disclose.

Correspondence: Vincent M. Borderie, Service V, Centre Hospitalier National d'Ophtalmologie des 15-20, 28 rue de Charenton, 75571 Paris, France (e-mail: vincent.borderie@upmc.fr).

low-coherence interferometry.[15] The high axial resolution allows precise delineation of corneal surfaces to be obtained. SD-OCT can provide accurate corneal ET mapping[5,16] with good reliability and repeatability.[17,18] However, anterior segment SD-OCT has become an important tool for characterizing the morphological changes in several corneal diseases.[19]

We hypothesized that analysis of SD-OCT epithelial maps could provide relevant information for the diagnosis of several ocular surface disorders. Therefore, our study aimed to analyze the value of corneal ET mapping in the diagnosis of ocular surface disorders involving the corneal epithelium and to correlate ET patterns and pathologies. We also evaluated the reproducibility of the pattern classification.

METHODS

Study Design

This study was a retrospective comparative study performed in a national tertiary center (Centre Hospitalier National d'Ophtalmologie des Quinze-Vingts, Paris, France) between January 2013 and September 2020. It was approved by the Ethics Committee of the French Society of Ophthalmology. Described research adhered to the tenets of the Declaration of Helsinki.

The study group was designed from records of a consecutive series of patients with a confirmed diagnosis. Data were recorded retrospectively. The study group consists of eyes with an ocular surface disorder involving the corneal epithelium and OCT assessment. The inclusion criteria were diagnosis confirmed by a senior cornea subspecialist (V.M.B.) and high-quality OCT images acquired by 1 experienced orthoptist (C.G.). Three hundred three eyes of 303 patients were included. We selected the following 7 ocular surface disorders affecting the corneal epithelium with different physiopathological mechanisms: keratoconus, LSCD, EBMD, dry eye, pterygium, trachoma, and in situ carcinoma. The numbers of eyes included in each group reflect the usual practice in our institution, that is, the percentages of patients with various disorders routinely examined in our corneal and external eye disease department. The diagnosis was based on medical history, ocular symptoms, slitlamp examination using fluorescein staining, SD-OCT scans, and corneal topography data.

Clinical features of keratoconus included corneal ectasia, apical thinning, Vogt striae, Fleischer ring, Munson sign, Rizzuti sign, or corneal scarring consistent with keratoconus. The diagnosis of keratoconus was facilitated by the use of corneal tomographic data (Oculus, Pentacam, OCULUS GmbH, Wetzlar, Germany): keratoconus appearance on the topography (skewed asymmetric bowtie, central or inferior steep zone, or claw shape) and positive topographic indices (mean keratometry >47 diopters or inferior–superior value >1.4 diopters in the central 3.0 mm according to the Rabinowitz and McDonnell criteria).[20] We did not use the grade of severity to analyze subgroups, but all stages of severity were included except forme fruste keratoconus and pregraft keratoconus. The mean keratometry was >47 and <55 diopters (stages 1–3 from the Krumeich classification). Clinical features of LSCD included late fluorescein staining, superficial corneal vascularization, epithelial opacities, and recurrent epithelial defects. The diagnosis of LSCD was confirmed in all cases with at least 2 of the following tests: IVCM; SD-OCT of the limbus with parallel, perpendicular, and en face sections; and histology of the tissue retrieved at the time of limbal stem cell transplantation. The different etiologies selected were chemical burns (n = 15), severe allergic keratoconjunctivitis (n = 6), congenital aniridia (n = 13), long-standing contact lens wear (n = 13), Lyell syndrome (n = 4), chemotherapy (n = 2), and multiple eye surgeries with a history of herpes zoster infection (n = 3). Clinical features of EBMD included subepithelial fingerprint lines, geographic maps, microcysts, and epithelial dots. Patients with EBMD presented symptomatic recurrent corneal erosions. SD-OCT scan features of EBMD included the presence of irregular and thickened epithelial basement membrane duplicating and/or insinuating into the corneal epithelium layer, presence of hyperreflective dots, and hyporeflective spaces between the corneal epithelial layer and the Bowman layer.[21] Dry eyes were diagnosed by the association of ocular symptoms for more than 3 months, tear film abnormalities (tear film break-up time <10 seconds and 3-minute Schirmer test <10 mm) with ocular surface damage (corneal or conjunctival staining with fluorescein, using the Oxford Scheme).[22] Different etiologies were selected: primary Sjögren syndrome (n = 6) and meibomian gland dysfunction (n = 15). No treatments of dryness were introduced before SD-OCT assessment (neither eye drops nor systemic treatments). The diagnosis of pterygium was based on the slitlamp findings. The suspected lesions of in situ carcinoma were presented as elevated lesions with a leukoplakic, gelatinous, or papilliform appearance, usually in the limbal area. The diagnosis of in situ carcinoma was further confirmed by histopathology. The diagnosis of trachoma was based on the medical history (history of trachoma in childhood) and the presence of corneal opacities.

When both eyes were involved, only the most affected one was included. Exclusion criteria were a history of corneal or intraocular surgery; contact lens wear; associated corneal disorders; associated ocular pathologies such as macular degeneration, retinopathy, and glaucoma; or a history of retinal detachment.

The control group consists of normal eyes with OCT assessment. The inclusion criteria were as follows: the absence of ocular symptoms and eye disease, no contact lens wear, no history of ocular surgery or trauma, normal slitlamp examination, normal ocular surface testing (ie, tear film break-up time >10 seconds and 3-minute Schirmer test >10 mm), and normal SD-OCT scans. Fifty-five eyes of 55 patients were included.

Data Collection

Demographic data, medical history, slitlamp findings, and spectral domain optical coherence tomography examination findings were recorded.

Spectral Domain Optical Coherence Tomography

We acquired 6-mm-wide SD-OCT scans (Optovue RTVue-100; Optovue Inc, Fremont, CA) with the long corneal adapter module in the center of the cornea. Scans had an axial resolution of 5 μm and a transverse resolution of 15 μm. The corneal adapter module software automatically processes the OCT scans to provide the ET map in the central 6 mm. For each eye, central ET; superior, inferior, nasal, and temporal epithelial thicknesses; and epithelial statistics within the central 6-mm zone (minimum and maximal thicknesses, Max–Min, and SD) were recorded.

Classification of ET Profiles

Based on the color-coded ET maps, we established a classification of 14 different ET patterns as follows: normal, spoke-wheel, central thickening, inferior thickening, superior thickening, nasal thickening, temporal thickening, diffuse thickening, doughnut (a localized central thinning with a ring of thick epithelium), central thinning, inferior thinning, superior thinning, diffuse thinning, and peripheral annular thinning patterns. Figure 1 shows the 14 patterns. Patterns were not exclusive to each other; that is, 1 eye could feature more than 1 pattern. Three trained physicians were involved in reviewing all the pachymetry maps and classifying the patterns for each image in a masked fashion.

Statistical Analysis

Qualitative (ET pattern) and quantitative (ET data) variables were analyzed, respectively, with the χ^2 test and analysis of variance with appropriate post hoc tests. The Spearman rank correlation coefficient was used to assess the effect of aging on quantitative variables. When quantitative variables were shown to be significantly associated with a given corneal condition in the post hoc test, receiving operating curves were used to determine the diagnostic threshold values. The observations from the control group and each disease group were randomly separated into a training set and a validation set. The receiver operating curve (ROC) analysis was performed using data from the control group and from the analyzed disease group, that is, the quantitative variable was assessed for its ability to distinguish corneas with the given disorder from normal ones. The training set was used to determine the threshold value of the quantitative variable and the validation set for calculating the area under the curve (AUC) associated with the threshold value. Finally, sensitivity and specificity of ET pattern and data were calculated for each disease group using all observations to assess the ability to distinguish corneas with a given corneal disorder from other conditions including diseased and normal corneas.

RESULTS

We included 303 eyes in the study group: keratoconus (135 eyes), LSCD (56 eyes), EBMD (55 eyes), dry eye (21

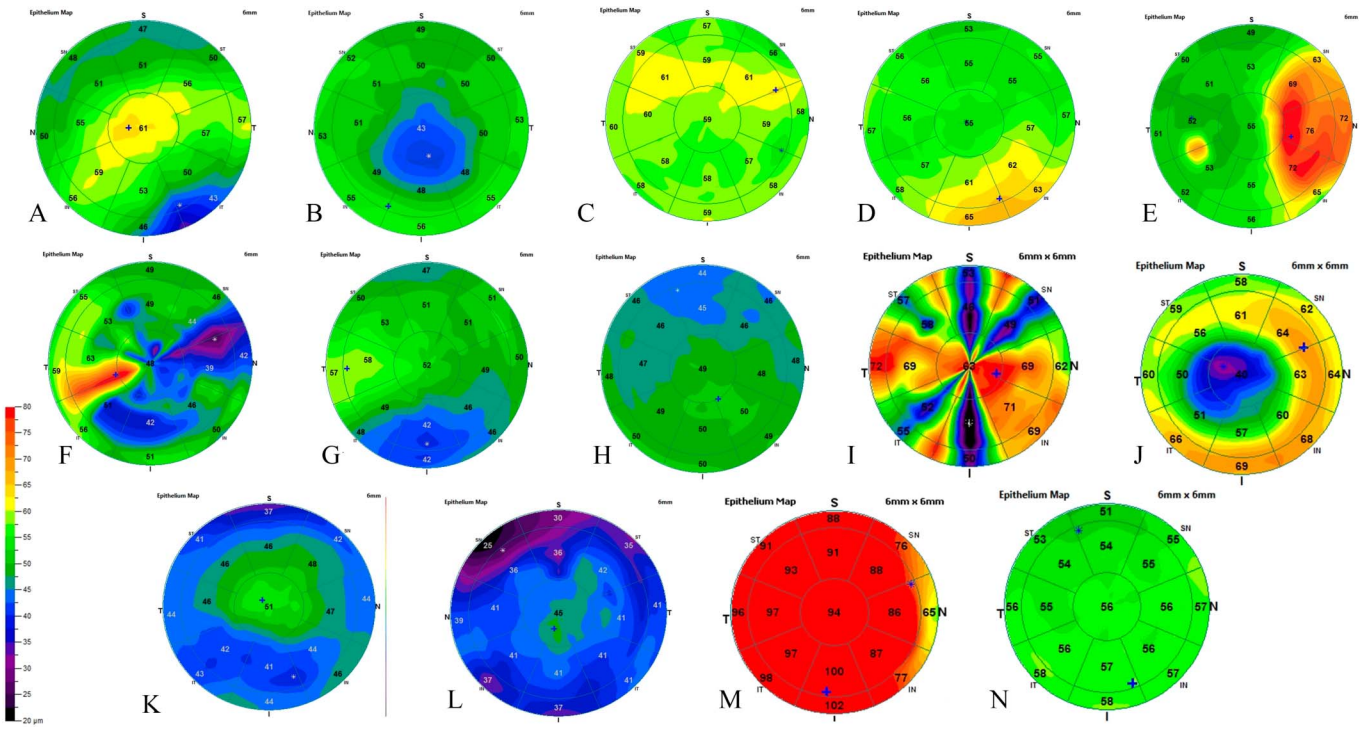

FIGURE 1. Examples of the 14 patterns described in epithelial mapping. A, Central thickening. B, Central thinning. C, Superior thickening. D, Inferior focal thickening. E, Nasal thickening. F, Temporal thickening. G, Inferior thinning. H, Superior thinning. I, Spoke-like pattern. J, Doughnut aspect. K, Peripheral concentric thinning. L, Diffuse thinning. M, Diffuse thickening. N, Normal.

eyes), pterygium (10 eyes), trachoma (15 eyes), and in situ carcinoma (11 eyes) and 55 eyes in the control group.

Patient Age

The mean (±SD) patient age in the different groups was as follows: control, 38 ± 16 years (range, 18–86 years); keratoconus, 35 ± 13 years (11–79 years); LSCD, 46 ± 16 years (16–75 years); EBMD, 58 ± 14 years (26–85 years); dry eye, 57 ± 15 years (30–76 years); pterygium, 66 ± 14 years (45–84 years); trachoma, 72 ± 10 years (58–88 years); and in situ carcinoma, 70 ± 12 years (50–88 years).

Corneal Epithelial Mapping Characteristics of the Different OSDs

Reproducibility of corneal epithelial map classification: Full agreement between the 3 readers (ie, 3 identical classifications) was obtained in 75.4% to 99.4% of cases depending on the following patterns: spoke-wheel pattern, 94.3%; central thickening, 96.6%; inferior/superior thickening, 87.8%; nasal/temporal thickening, 93.1%; diffuse thickening/thinning, 99.4%; doughnut pattern, 75.4%; central thinning, 92.6%; inferior/superior thinning, 88.0%; and peripheral annular thinning, 89.7%. Cases with a noncomplete agreement were re-evaluated by the 3 readers working together.

Table 1 shows the qualitative analysis of the corneal ET mapping in the 10 groups of patients. Several ocular surface disorders (OSDs) were significantly associated with an ET mapping pattern as follows: keratoconus with the doughnut pattern (sensitivity, 56% and specificity, 94%), the inferior thinning pattern (47% and 96%), limbal deficiency with the spoke-wheel pattern (66% and 98%), EBMD with the inferior thickening pattern (55% and 92%), dry eye with the superior thinning pattern (67% and 88%), and pterygium with the nasal thickening pattern (100% and 86%).

Table 2 shows the quantitative analysis of the corneal ET mapping in the 10 groups of patients. When analysis of variance (ANOVA) with the appropriate post hoc test showed that quantitative ET data could significantly discriminate a given OSD from normal corneas, ROC analysis was used to quantify accuracy (Table 3). Threshold values were determined using the training set, and the AUC was assessed in the validation set. Several ET variables featured high accuracy in distinguishing OSD corneas from controls. Specificity was at least 90% for most ET variables. It was higher than sensitivity for all these variables but one, that is, their ability to eliminate the OSD diagnosis was stronger than their ability to confirm the OSD diagnosis. The AUC was greater than 0.90 in 12 of 34 cases. When the threshold values were used to distinguish each group from the remaining diseased and control groups, specificity decreased below 85% for most ET variables. However, decreased temporal and nasal ETs as markers of limbal deficiency were still associated with specificity greater than 85%.

In summary, the main features of the ocular surface disorders obtained with epithelial map classification and ET data were as follows:

1. Keratoconus: doughnut pattern (sensitivity/specificity = 56/94%), inferior thinning pattern (47/96%), max–min ET ≥ 13 μm (84/43%), and ET SD > 5 μm (47/58%).
2. LSCD: spoke-wheel pattern (66/98%), max–min ET ≥ 14 μm (91/59%), ET SD > 5 μm (82/63%), and minimal ET ≤ 43 μm (88/58%).
3. EBMD: inferior thickening pattern (55/92%), ET SD > 5 μm (67/58%), and central ET > 56 μm (53/81%).
4. Dry eye: superior thinning pattern (67/88%) and minimal ET ≤ 44 μm (86/47%).
5. Pterygium: nasal thickening pattern (100/86%), nasal ET > 56 μm (80/71%), max–min ET ≥ 19 μm (100/50%), and ET SD >5 μm (70/57%).
6. Trachoma: max–min ET ≥ 15 μm (100/38%) and min ET ≤ 44 μm (73/46%).
7. In situ carcinoma: max ET > 60 μm (91/60%), ET SD > 5 μm (100/58%), and max–min ET ≥ 22 μm (73/56%).

Effect of Aging on ET Characteristics

When all groups were considered, increased age was significantly associated with increased central ($r_s = 0.12$), max ($r_s = 0.13$), and max–min ($r_s = 0.12$) ETs and decreased superior ($r_s = -0.15$) ETs. In the control group, increased age was significantly associated with increased max ET ($r_s = 0.30$) and increased ET variability (max–min, $r_s = 0.51$ and SD, $r_s = 0.55$).

Stratification on Age

Because significant age differences were observed between groups, a stratified analysis was performed based on age. The observations were divided into 2 age groups as follows: 40 years or younger and older than 40 years. For quantitative variables, stratified analysis was performed for variables correlated with age (Table 4). Stratification on the age group did not modify the results of post hoc tests, except for the superior and max–min ETs that were no longer significant in dry eyes. For qualitative variables, stratified analysis was performed for all variables as all patterns were dependent on the age group (data not shown). Stratification on the age group did not modify the results of chi-square tests, except for the superior and diffuse thickening patterns that were significant only in patients older than 40 years.

DISCUSSION

Our study design was close to real-life practice with a repartition of disorders resembling that observed in routine practice in our institution. We first demonstrated that ET patterns and data were relevant for distinguishing diseased from normal corneas. Finally, we showed that patterns and several ET data were useful to distinguish diseased corneas among a panel of normal and abnormal corneas as observed in real life. Our proposed diagnosis method is highly objective because pattern classification was found to be

TABLE 1. Qualitative Analysis of Corneal ET Mapping in the 7 Groups of Patients With OSDs and Controls

	Controls	Keratoconus	Limbal Deficiency	EBMD	Dry Eye	Pterygium	Trachoma	In Situ Carcinoma	Chi-Square Test *P*
No. of eyes	55	135	56	55	21	10	15	11	
Spoke-wheel pattern	0	3	**37** **Se/Sp = 66/ 98%**	0	0	0	2	1	<0.0001
Central thickening	0	14	9	14 Se/Sp = 25/ 90%	1	4 Se/Sp = 40/ 88%	1	3 Se/Sp = 27/ 88%	<0.0001
Inferior thickening	0	8	2	**30** **Se/Sp = 55/ 92%**	5 Se/Sp = 28/ 85%	4 Se/Sp = 40/ 86%	1	4 Se/Sp = 36/ 86%	<0.0001
Superior thickening	0	13	2	13 Se/Sp = 24/ 94%	0	1	1	2	0.01
Nasal thickening	0	32 Se/Sp = 24/ 88%	2	9	1	**10** **Se/Sp = 100/ 86%**	1	5 Se/Sp = 45/ 84%	<0.0001
Temporal thickening	2	56 Se/Sp = 41/ 90%	4	9	1	2 Se/Sp = 20/ 77%	1	4 Se/Sp = 36/ 78%	<0.0001
Diffuse thickening	0	2	1	4	0	3 Se/Sp = 30/ 97%	2	3 Se/Sp = 27/ 97%	<0.0001
Doughnut pattern	0	**76** **Se/Sp = 56/ 94%**	5	3	3	1	2	0	<0.0001
Central thinning	0	24	4	0	5	0	0	1	0.0001
Inferior thinning	0	63 Se/Sp = 47/ 96%	4	2	2	0	0	1	<0.0001
Superior thinning	0	12	9	8	**12** **Se/Sp = 67/ 88%**	4 Se/Sp = 40/ 86%	3 Se/Sp = 20/ 86%	3 Se/Sp = 27/ 86%	<0.0001
Diffuse thinning	0	0	4	0	1	0	4 Se/Sp = 27/ 99%	0	<0.0001
Peripheral annular thinning	0	4	13 Se/Sp = 23/ 98%	1	2	0	0	1	<0.0001

Shown are the numbers of eyes with the corresponding patterns in each of the 8 groups of patients. One eye may feature more than 1 pattern.

The *P* values refer to the overall comparison. Sensitivity and specificity were calculated using all 8 groups. Shown are Se/Sp for patterns with Se > 20%. Data in bold correspond to sensitivity >50%.

Se/Sp, sensitivity/specificity.

repeatable among different observers, and ET data and statistics are provided by the SD-OCT device.

In this study, several patterns were significantly and specifically associated with OSDs, that is, doughnut pattern and keratoconus (sensitivity/specificity = 56/94%), spoke-wheel pattern and LSD (66/98%), superior thinning pattern and dry eye (67/88%), inferior thickening pattern and EBMD (55/92%), and nasal thickening pattern and pterygium (100/86%).

The normal corneal epithelium features a nonuniform pattern, and it tends to alter its pattern for the compensation of stromal irregularities. In 1993, Simon et al1 suggested that the epithelium does not form a uniform layer. It was further confirmed by Reinstein et al[14] who described the corneal ET profile over a 10-mm diameter area in a population of normal eyes (with an ultrasound device): On average, the ET is, at the vertex, 53.4 ± 4.6 μm; it is 5.7 μm thicker in the 3-mm inferior epithelium than in the 3-mm superior epithelium and 1.2 μm thicker in the 3-mm nasal epithelium than the 3-mm temporal epithelium. In our study, in normal eyes, we observed a central ET of 52.8 ± 2.9 μm and an epithelium slightly thicker inferiorly (53.3 ± 3.3 μm) and nasally (52.4 ± 3.1 μm). This nonuniform thickness profile was suggested to be induced by the mechanical friction of the

TABLE 2. Quantitative Analysis of Corneal ET Mapping in the 7 Groups of Patients With OSDs Compared With the Control Group

	Controls	Keratoconus	Limbal Deficiency	EBMD	Dry Eye	Pterygium	Trachoma	In Situ Carcinoma	ANOVA *P*
No. of eyes	55	135	56	55	21	10	15	11	
Central ET	52.8 ± 2.9	50.8 ± 6.0	51.7 ± 10.7	**58.2 ± 6.8**	50.2 ± 6.5	55.0 ± 5.4	55.3 ± 14.8	**60.7 ± 13.9**	<0.0001
Minimal ET	49.1 ± 3.3	***40.9 ± 7.1***	***28.3 ± 15.1***	47.6 ± 6.6	***42.6 ± 5.1***	45.3 ± 3.5	***38.0 ± 14.3***	44.0 ± 19.9	<0.0001
Maximal ET	56.3 ± 4.0	**62.9 ± 6.8**	**68.6 ± 14.9**	**66.8 ± 10.0**	58.2 ± 8.8	74.0 ± 7.3	**70.4 ± 13.3**	**75.5 ± 16.6**	<0.0001
Temporal ET	51.9 ± 2.9	52.8 ± 5.9	***47.3 ± 14.5***	**55.3 ± 5.7**	49.2 ± 4.8	50.4 ± 4.2	51.6 ± 10.6	**63.3 ± 19.5**	<0.0001
Nasal ET	52.4 ± 3.1	**55.3 ± 5.2**	***48.2 ± 13.8***	**55.7 ± 5.9**	50.2 ± 7.4	**63.1 ± 11.8**	48.6 ± 12.4	**57.5 ± 10.3**	<0.0001
Superior ET	51.8 ± 3.0	52.6 ± 5.3	***45.7 ± 14.2***	52.4 ± 6.8	***47.0 ± 6.0***	48.7 ± 5.5	50.7 ± 9.8	54.3 ± 15.1	<0.0001
Inferior ET	53.3 ± 3.3	53.5 ± 6.4	***49.3 ± 11.6***	**58.6 ± 7.5**	52.9 ± 8.0	53.1 ± 5.7	53.3 ± 12.2	**63.3 ± 16.0**	<0.0001
Max–min ET	7.3 ± 3.9	**21.9 ± 10.8**	**40.3 ± 18.9**	**19.2 ± 12.0**	**15.6 ± 9.5**	**28.8 ± 7.7**	**32.5 ± 14.8**	**31.5 ± 18.1**	0.01
ET SD	1.6 ± 0.9	**5.4 ± 2.7**	**11.2 ± 14.7**	**4.5 ± 2.8**	3.9 ± 2.7	**6.5 ± 3.0**	**6.8 ± 2.8**	**7.3 ± 4.1**	<0.0001

Shown is mean ± SD. Data in bold are significantly higher (only bold) or lower (bold and italic) compared with the control group in post hoc tests.

upper eyelid on the superior region, during blinking, damaging epithelial cells and resulting in epithelial thinning.[23]

LSCD was associated with a spoke-wheel pattern, a max–min ET greater than 14 μm, and an ET SD greater than 5 μm. These findings are consistent with our previous study.[9] Indeed, the difference between the minimal and maximal ETs and the ET variability were significantly higher in eyes with LSCD than in normal eyes, whereas there was no difference in central ET between both groups. Conversely, Liang et al[10] reported that the reduction of central ET was more than 20%

TABLE 3. Threshold Value, AUC, Sensitivity, and Specificity of ET Features Significantly Associated With OSDs

	Keratoconus	Limbal Deficiency	EBMD	Dry Eye	Pterygium	Trachoma	In Situ Carcinoma
Central ET			T > 56 μm AUC = 0.79 Se/Sp = 53/81%				
Minimal ET	T ≤ 44 μm AUC = 0.86 Se/Sp = 68/53%	**T ≤ 43 μm** AUC = 0.91 Se/Sp = 88/58%		T ≤ 44 μm AUC = 0.88 Se/Sp = 86/47%		T ≤ 44 μm AUC = 0.88 Se/Sp = 73/46%	
Maximal ET	T > 59 μm AUC = 0.82 SeSp = 67/45%	T > 62 μm AUC = 0.76 Se/Sp = 63/58%	T > 60 μm AUC = 0.87 Se/Sp = 76/49%			T > 62 μm AUC = 0.84 Se/Sp = 73/56%	**T > 60 μm** AUC = 0.96 Se/Sp = 91/60%
Temporal ET		T ≤ 45 μm AUC = 0.66 Se/Sp = 57/91%	T > 55 μm AUC = 0.70 Se/Sp = 45/76%				
Nasal ET	T > 55 μm AUC = 0.70 Se/Sp = 46/68%	T ≤ 48 μm AUC = 0.61 Se/Sp = 48/88%	T > 56 μm AUC = 0.68 Se/Sp = 47/73%		T > 56 μm AUC = 0.80 Se/Sp = 80/71%		
Superior ET		T ≤ 47 μm AUC = 0.68 Se/Sp = 59/81%		T ≤ 45 μm AUC = 0.73 Se/Sp = 48/85%			
Inferior ET		T ≤ 48 μm AUC = 0.68 Se/Sp = 54/83%	T > 57 μm AUC = 0.75 Se/Sp = 56/81%				T > 57 μm AUC = 0.79 Se/Sp = 64/76%
Max–min ET	**T ≥ 13 μm** AUC = 0.94 Se/Sp = 84/43%	**T ≥ 14 μm** AUC = 0.97 Se/Sp = 91/58%	T ≥ 10 μm AUC = 0.89 Se/Sp = 82/20%	T ≥ 7 μm AUC = 0.85 Se/Sp = 95/11%	**T ≥ 19 μm** AUC = 0.99 Se/Sp = 100/50%	**T ≥ 15 μm** AUC = 0.99 Se/Sp = 100/38%	**T ≥ 22 μm** AUC = 0.91 Se/Sp = 73/56%
ET SD	**T > 5 μm** AUC = 0.96 Se/Sp = 47/58%	**T > 5 μm** AUC = 0.96 Se/Sp = 82/63%	**T > 5 μm** AUC = 0.97 Se/Sp = 67/58%		**T > 5 μm** AUC = 0.98 Se/Sp = 70/57%	T > 3 μm AUC = 0.85 Se/Sp = 100/59%	**T > 5 μm** AUC = 1.00 Se/Sp = 100/58%

Only variables that were significant in the ANOVA post hoc test were analyzed with ROCs. ROC analysis was performed for each study group versus the control group to determine the threshold value and its ability to distinguish the given ocular surface disorder from normal eyes (AUC). Threshold values were determined using the training set, and AUC was assessed in the validation set. Sensitivity and specificity were calculated with all observations (n = 358) to assess the test ability to distinguish the given disorder from all other conditions.

Se/Sp, sensitivity/specificity; T, threshold value.

TABLE 4. Comparison of the 7 Groups of Patients With OSDs With the Control Group After Stratification on Age

		Keratoconus	Limbal Deficiency	EBMD	Dry Eye	Pterygium	Trachoma	In Situ Carcinoma
Central ET	All	0.10 (135)	0.42 (56)	**0.0002 (55)**	0.18 (21)	0.41 (10)	0.26 (15)	**0.002 (11)**
	Age <40 yrs	0.13 (91)	0.95 (18)	**0.004 (7)**	— (2)	— (0)	— (0)	— (0)
	Age >40 yrs	0.31 (44)	0.40 (38)	**0.04 (48)**	0.25 (19)	0.63 (10)	0.51 (15)	**0.02 (11)**
Maximal ET	All	**<0.0001 (135)**	**<0.0001 (56)**	**<0.0001 (55)**	0.45 (21)	**<0.0001 (10)**	**<0.0001 (15)**	**<0.0001 (11)**
	Age <40 yrs	**<0.0001 (91)**	**<0.0001 (18)**	**<0.0001 (7)**	— (2)	— (0)	— (0)	— (0)
	Age >40 yrs	0.22 (44)	**0.001 (38)**	**0.006 (48)**	0.84 (19)	**0.0003 (10)**	**0.002 (15)**	**<0.0001 (11)**
Superior ET	All	0.50 (135)	**<0.0001 (56)**	0.68 (55)	**0.02 (21)**	0.25 (10)	0.62 (15)	0.33 (11)
	Age <40 yrs	0.42 (91)	**<0.0001 (18)**	0.67 (7)	– (2)	— (0)	— (0)	— (0)
	Age >40 yrs	0.83 (44)	**0.02 (38)**	0.76 (48)	0.10 (19)	0.41 (10)	0.76 (15)	0.42 (11)
Max–min ET	All	**<0.0001 (135)**	**<0.0001 (56)**	**<0.0001 (55)**	**0.008 (21)**	**<0.0001 (10)**	**<0.0001 (15)**	**<0.0001 (11)**
	Age <40 yrs	**<0.0001 (91)**	**<0.0001 (18)**	**0.0008 (7)**	— (2)	— (0)	— (0)	— (0)
	Age >40 yrs	**0.001 (44)**	**<0.0001 (38)**	**0.01 (48)**	0.25 (19)	**0.0004 (10)**	**<0.0001 (15)**	**<0.0001 (11)**

Shown is the *P* value of post hoc tests and the number of eyes for variables significantly correlated with age.

in LSCD eyes, and this reduction increased with the number of affected limbal and corneal regions. Central ET could reflect the global function of limbal stem cells. In this study, we did not grade the stages of LSCD. This could be a limit for the interpretation of the central ET because the hyperreflective subepithelial fibrosis can interfere with the ET measurements (with the precise location of the epithelial layer and Bowman layer),[9] which probably results in ET overestimation. Our previous study showed the presence of subepithelial fibrosis in 76% of the eyes with LSCD and none of the normal eyes.

Keratoconus was associated with a doughnut pattern, an inferior thinning pattern, and a max–min ET greater than 13 μm. No significant differences in central ET were observed between keratoconus eyes and controls. These findings are consistent with the data published in 2012, when Li et al5 reported a central ET around 51.9 ± 5.3 μm in 35 keratoconus eyes and around 52.3 ± 3.6 μm in normal eyes, with no significant differences between both groups. On the other hand, Pircher et al[24] observed a significant reduction of central ET in keratoconus eyes around 9.2% of the normal cornea. These data confirmed what Haque et al[25] already reported: a reduction of 4.7 μm in central ET in keratoconus eyes compared with controls.

Reinstein et al[26] suggested that epithelial changes may allow an earlier diagnosis of keratoconus because the epithelial changes appear before the changes on the front surface of the cornea. The epithelial remodeling appears to smooth and reduce the bulging of the anterior stromal surface.[26] The epithelial doughnut pattern was then described, defined by epithelial thinning surrounded by an annulus of thicker epithelium, colocalized with an eccentric posterior elevation best-fit sphere apex. An epithelial doughnut pattern appears to indicate the presence of an underlying stromal cone. In our study, 56% of the keratoconus had an epithelial doughnut pattern. Li et al[5] reported that the epithelial profile in all keratoconus eyes is a thinning of the inferotemporal epithelium and a thickening of the superonasal epithelium. We also observed a similar pattern in our results: 47% had an inferior thinning. In most keratoconus eyes, we observe the cone apex in the central 5-mm diameter of the cornea,[27] so the central thinning of the doughnut pattern can be detectable with a 6-mm-wide OCT scans. However, it is possible that the central 6-mm zone, as used here, is not wide enough to observe all epithelial changes, especially that a full ring of thicker epithelium can be missed.

Dry eye was associated with a superior thinning pattern and a minimal ET lower than 44 μm in our series. Cui et al[28] reported a thinner superior ET compared with normal eyes. They reported a weak correlation between thinned superior epithelium and decreased Schirmer test. The superior epithelium in grade 4 of dryness was significantly thinner than in grade 1. The supposed mechanism is an increase of blinking to compensate for the tear deficiency. This mechanical friction intensifies the epithelium damage and makes the superior epithelium thinner.

The nonsignificant difference in central ET between dry eyes and controls is consistent with previous results reported by Francoz et al[29] and Liang.[30] It has been proven that ET is more altered in peripheral regions than in the central region[29] and that its alteration is more enlarged in severely dry eyes.[28] However, Kanellopoulos et al[16] reported a thicker central ET, whereas El Fayoumi et al[31] reported a thinner central ET. The inclusion of different stages and causes of dryness might have contributed to these various results: The inflammatory process induces epithelial proliferation,[32] whereas an impaired subbasal nerve plexus results in corneal epithelial thinning.[33]

In our study, both the central and inferior ETs were significantly increased in EBMD eyes. These results are consistent with what Buffault et al8 previously reported: The ET in EBMD was significantly thicker compared with normal eyes, except for the superior and minimal ETs. The suggested mechanism is the mechanical friction of the upper lid on a more fragile epithelium.[8] Histologically, in EBMD, the basement membrane is thickened and multilamellar, and the hemidesmosomes are nonfunctional: There is a lack of adhesion of the epithelial cells on the basement membrane.[34,35] However, the corneal epithelium could be pushed down from the superior to the inferior region and accumulate in the inferior region, resulting in a thickening of the epithelium. In this study, the inferior thickening pattern was significantly associated with EBMD with 92% specificity.

A few studies reported the ET in in situ carcinoma. In 2017, Atallah et al[36] evaluated the role of HR-OCT in 16 patients with ocular surface squamous neoplasia (OSSN) and a coexisting ocular disease and lesions potentially suspicious for OSSN. OCT scan features suggesting OSSN were epithelial thickening and hyperreflectivity. The OSSN diagnosis was confirmed by biopsies. Although the gold standard for the diagnosis of carcinoma remains to be histopathological, the finding of epithelial thickening in patients with clinical suspicion of carcinoma can be helpful in the orientation of the diagnosis. Our study provides quantitative thresholds for both max ET (60 μm) and inferior ET (57 μm).

A strong correlation between the location of pterygium and the location of the epithelial thickening was found in this study with all pterygia being located nasally and associated with nasal thickening in ET maps.

Age was significantly correlated with several quantitative variables, and ET map pattern was dependent on patient age. The stratified analysis did not lead to substantial changes in the results of statistical analysis, and it did not affect the main features of the ocular surface disorders obtained with epithelial map classification and ET data.

Our retrospective case–control series has some limitations including its retrospective design. The number of eyes included in some groups is low, and this could decrease the statistical power of our results. Another limitation is the limited 6-mm diameter size of the thickness map. Some patterns could have been underestimated; for instance, a full ring of thickness surrounding an epithelial thinning might have been missed. A larger map size would help to differentiate some patterns for disorders involving the peripheral cornea. We did not grade the severity of patients with dry eye, LSCD, and keratoconus. Because we included only high-quality OCT images, a selection bias cannot be ruled out. Our study was based on a given spectral domain OCT device, and our results and conclusions cannot be transposed to other OCT devices because measurements can be device-dependent. A possible source of uncertainty in our study is the tear film discrimination inability. The ET provided by the current SD-OCT Optovue RTVue-100 incorporates the tear film. This can explain why in our study we found ET thicker than others using ultrahigh-resolution OCT.[37,38] Optovue RTVue-100 has an axial resolution of 5 μm, whereas other anterior SD-OCTs have a better axial resolution (for example, around 3.9 μm for the SPECTRALIS OCT, Heidelberg, Germany) and do not include the tear film in the ET measurement. The tear film is seen as the first hyperreflective layer and the basal membrane as the second hyperreflective layer.[39] Finally, in severe stages in both LSCD and keratoconus, a stromal scar can interfere with the automatic epithelial mapping of the device that could lead to inaccurate measurements. The SD-OCT device tends to consider the posterior limit of superficial scars as the epithelial basement membrane, leading to overestimation of the ET in these cases. Manually, we can measure the true ET using the calipers provided by the SD-OCT device, but we still miss automatized methods to measure it.

CONCLUSIONS

Whereas distinguishing corneas with a given ocular surface condition from normal corneas is relatively easy to achieve with a quantitative biomarker analyzed with ROCs, the diagnosis of several conditions among eyes with various conditions is still difficult to achieve even with advanced artificial intelligence technologies. In this study, we show that epithelial map pattern recognition combined with quantitative analysis of ET using threshold values determined by ROCs may help the clinician in diagnosing various ocular surface conditions and distinguishing them from each other. The last step of the precise diagnosis has still to be made by the clinician. However, deep learning analysis of big data could lead to the fully automated diagnosis of these ocular surface conditions.

REFERENCES

1. Simon G, Ren Q, Kervick GN, et al. Optics of the corneal epithelium. *Refract Corneal Surg.* 1993;9:42–50.
2. Reinstein DZ, Silverman RH, Sutton HF, et al. Very high-frequency ultrasound corneal analysis identifies anatomic correlates of optical complications of lamellar refractive surgery: anatomic diagnosis in lamellar surgery. *Ophthalmology*. 1999;106:474–482.
3. Reinstein DZ, Archer TJ, Gobbe M, et al. Epithelial thickness after hyperopic LASIK: three-dimensional display with artemis very high-frequency digital ultrasound. *J Refract Surg.* 2010;26:555–564.
4. Vogt A. Atlas of the slitlamp-microscopy of the living eye. *Surv Ophthalmol.* 1962;7:316–321.
5. Li Y, Tan O, Brass R, et al. Corneal epithelial thickness mapping by Fourier-domain optical coherence tomography in normal and keratoconic eyes. *Ophthalmology*. 2012;119:2425–2433.
6. Reinstein DZ, Archer TJ, Gobbe M. Corneal epithelial thickness profile in the diagnosis of keratoconus. *J Refract Surg.* 2009;25:604–610.
7. Temstet C, Sandali O, Bouheraoua N, et al. Corneal epithelial thickness mapping using Fourier-domain optical coherence tomography for detection of form fruste keratoconus. *J Cataract Refract Surg.* 2015; 41:812–820.
8. Buffault J, Zéboulon P, Liang H, et al. Assessment of corneal epithelial thickness mapping in epithelial basement membrane dystrophy. *PLoS One*. 2020;15:e0239124.
9. Banayan N, Georgeon C, Grieve K, et al. Spectral-domain optical coherence tomography in limbal stem cell deficiency. A case-control study. *Am J Ophthalmol.* 2018;190:179–190.
10. Liang Q, Le Q, Cordova DW, et al. Corneal epithelial thickness measured using anterior segment optical coherence tomography as a diagnostic parameter for limbal stem cell deficiency. *Am J Ophthalmol.* 2020;216:132–139.
11. Li HF, Petroll WM, Møller-Pedersen T, et al. Epithelial and corneal thickness measurements by in vivo confocal microscopy through focusing (CMTF). *Curr Eye Res.* 1997;16:214–221.
12. Erie JC, Patel SV, McLaren JW, et al. Effect of myopic laser in situ keratomileusis on epithelial and stromal thickness: a confocal microscopy study. *Ophthalmology*. 2002;109:1447–1452.
13. Urs R, Lloyd HO, Reinstein DZ, et al. Comparison of very-high-frequency ultrasound and spectral-domain optical coherence tomography corneal and epithelial thickness maps. *J Cataract Refract Surg.* 2016;42: 95–101.
14. Reinstein DZ, Archer TJ, Gobbe M, et al. Epithelial thickness in the normal cornea: three-dimensional display with artemis very high-frequency digital ultrasound. *J Refract Surg.* 2008;24:571–581.
15. Huang D, Swanson EA, Lin CP, et al. Optical coherence tomography. *Science*. 1991;254:1178–1181.
16. Kanellopoulos AJ, Asimellis G. In vivo three-dimensional corneal epithelium imaging in normal eyes by anterior-segment optical coherence tomography: a clinical reference study. *Cornea*. 2013;32:1493–1498.
17. Sella R, Zangwill LM, Weinreb RN, et al. Repeatability and reproducibility of corneal epithelial thickness mapping with spectral-domain optical coherence tomography in normal and diseased cornea eyes. *Am J Ophthalmol.* 2019;197:88–97.

18. Sin S, Simpson TL. The repeatability of corneal and corneal epithelial thickness measurements using optical coherence tomography. *Optom Vis Sci.* 2006;83:360–365.
19. Werkmeister RM, Sapeta S, Schmidl D, et al. Ultrahigh-resolution OCT imaging of the human cornea. *Biomed Opt Express*. 2017;8:1221–1239.
20. Rabinowitz YS, McDonnell PJ. Computer-assisted corneal topography in keratoconus. *Refract Corneal Surg.* 1989;5:400–408.
21. El Sanharawi M, Sandali O, Basli E, et al. Fourier-domain optical coherence tomography imaging in corneal epithelial basement membrane dystrophy: a structural analysis. *Am J Ophthalmol.* 2015;159:755–763.
22. Bron AJ, Evans VE, Smith JA. Grading of corneal and conjunctival staining in the context of other dry eye tests. *Cornea*. 2003;22:640–650.
23. Reinstein DZ, Silverman RH, Trokel SL, et al. Corneal pachymetric topography. *Ophthalmology*. 1994;101:432–438.
24. Pircher N, Schwarzhans F, Holzer S, et al. Distinguishing keratoconic eyes and healthy eyes using ultrahigh-resolution optical coherence tomography-based corneal epithelium thickness mapping. *Am J Ophthalmol.* 2018;189:47–54.
25. Haque S, Jones L, Simpson T. Thickness mapping of the cornea and epithelium using optical coherence tomography. *Optom Vis Sci.* 2008;85: E963–E976.
26. Reinstein DZ, Gobbe M, Archer TJ, et al. Epithelial, stromal, and total corneal thickness in keratoconus: three-dimensional display with artemis very-high frequency digital ultrasound. *J Refract Surg.* 2010;26:259–271.
27. Tang M, Shekhar R, Miranda D, et al. Characteristics of keratoconus and pellucid marginal degeneration in mean curvature maps. *Am J Ophthalmol.* 2005;140:993–1001.
28. Cui X, Hong J, Wang F, et al. Assessment of corneal epithelial thickness in dry eye patients. *Optom Vis Sci.* 2014;91:1446–1454.
29. Francoz M, Karamoko I, Baudouin C, et al. Ocular surface epithelial thickness evaluation with spectral-domain optical coherence tomography. *Invest Ophthalmol Vis Sci.* 2011;52:9116–9123.
30. Liang Q, Liang H, Liu H, et al. Ocular surface epithelial thickness evaluation in dry eye patients: clinical correlations. *J Ophthalmol.* 2016; 2016:1628469.
31. El-Fayoumi D, Youssef MM, Khafagy MM, et al. Assessment of corneal and tear film parameters in rheumatoid arthritis patients using anterior segment spectral domain optical coherence tomography. *Ocul Immunol Inflamm.* 2018;26:632–638.
32. Fabiani C, Barabino S, Rashid S, et al. Corneal epithelial proliferation and thickness in a mouse model of dry eye. *Exp Eye Res.* 2009;89: 166–171.
33. Bouheraoua N, Hrarat L, Parsa CF, et al. Decreased corneal sensation and subbasal nerve density, and thinned corneal epithelium as a result of 360-degree laser retinopexy. *Ophthalmology*. 2015; 122:2095–2102.
34. Weiss JS, Møller HU, Lisch W, et al. The IC3D classification of the corneal dystrophies. *Cornea*. 2008;27(suppl 2):S1–S83.
35. Fogle JA, Kenyon KR, Stark WJ, et al. Defective epithelial adhesion in anterior corneal dystrophies. *Am J Ophthalmol.* 1975;79:925–940.
36. Atallah M, Joag M, Galor A, et al. Role of high resolution optical coherence tomography in diagnosing ocular surface squamous neoplasia with coexisting ocular surface diseases. *Ocul Surf.* 2017;15: 688–695.
37. Yadav R, Kottaiyan R, Ahmad K, et al. Epithelium and Bowman's layer thickness and light scatter in keratoconic cornea evaluated using ultrahigh resolution optical coherence tomography. *J Biomed Opt.* 2012;17:116010.
38. Tao A, Wang J, Chen Q, et al. Topographic thickness of Bowman's layer determined by ultra-high resolution spectral domain-optical coherence tomography. *Invest Ophthalmol Vis Sci.* 2011;52:3901–3907.
39. Wang J, Fonn D, Simpson TL, et al. The measurement of corneal epithelial thickness in response to hypoxia using optical coherence tomography. *Am J Ophthalmol.* 2002;133:315–319.